Closed Form Expression for the Cramér-Rao Lower Bound for the DOA Estimates from Spatially and Temporally Correlated Narrowband Signals Considering Noncircular Sources

Sonia Ben Hassen, and Abdelaziz Samet
Electronic Systems and Communication Networks Engineering
Tunisia Polytechnic School
La Marsa, Tunisia
Email: hassen@emt.inrs.ca, abdelaziz.samet@ept.rnu.tn

Faouzi Bellili, and Sofiène Affes
INRS-EMT
Montreal, Qc, H5A 1K6, Canada
Email: bellili@emt.inrs.ca, affes@emt.inrs.ca

***Abstract*—In this paper, we derive for the first time an explicit expression for the stochastic Cramér-Rao lower bound (CRLB or CRB) of the DOA estimates from spatially and temporally correlated signals generated from noncircular sources. The new CRB is compared to those of circular temporally correlated and noncircular independent and identically distributed (iid) signals. It will be shown that the CRB obtained assuming both noncircular sources and temporally correlated signals is lower than the CRBs derived considering only one of these two assumptions. This illustrates the potential gain that both the noncircularity and the temporal correlation provide when considered together. It will also be proved that the difference between the three CRBs increases with the number of snapshots. However, as the signal-to-noise ratio (SNR) increases, the CRBs merge together and decrease linearly. Moreover, we notice that in low SNR values the temporal correlation is more informative about the unknown DOA parameters than the noncircularity. Finally, we show the dependence of the CRB on the noncircularity rate, the noncircularity phase separation and the DOA separation.**

Keywords: DOA estimation, spatial correlation, temporal correlation, noncircularity of the signals, stochastic Cramér-Rao lower bound (CRLB).

I. INTRODUCTION

Direction of arrival (DOA) estimation for multiple plane waves impinging on an arbitrary array of sensors has received a significant amount of attention over the last several decades. It has typically played an important role in array signal processing areas such as modern wireless communication systems, radar, sonar, audio/speech processing systems and radio astronomy.

In this context, many DOA estimators have been extensively studied, assuming different data models. Indeed, a number of high resolution DOA estimation algorithms such as the deterministic (or conditional) and the unconditional Maximum Likelihood (ML) estimators [1], the MUltiple SIgnal Classification (MUSIC) estimator [2, 3] and the MODE estimator [4] have been developed assuming the signals to be independent and identically distributed (iid) and generated from circular sources. Moreover, efforts have been directed to devolop more realistic models assuming the signals to be temporally correlated and circular [5, 6]. Later, there was a considerable interest in diriving algorithms that exploit the unconjugated spatial covariance matrix for noncircular and iid signals [7, 8, 9].

The performance of any DOA estimator is often assessed by computing and plotting its bias and variance as a function of the true SNR values. In this context, a given unbiased estimator is usually said to outperform another one, over a given SNR range, if it has a lower variance.

In signal processing, a well known common lower bound for the variance of unbiased estimators of a given parameter is the Cramér-Rao Lower Bound (CRLB or CRB). It serves as a useful benchmark for practical estimators [10]. The CRLB is often numerically or empirically computed. But even when a closed-form expression can be obtained, it is usually complex and requires tedious algebraic manipulations. Roughly speaking, in signal processing, there are two major categories of DOA CRBs according to the transmitted signal: deterministic and stochastic. In the deterministic case, the transmitted signal is assumed to be an unknown deterministic process while in the stochastic case the transmitted signal is assumed to be stationary and generated from a random process. Because the derivation of the stochastic CRB was thought to be prohibitive in [1, (2.13)], the authors therein considered arbitrary deterministic signals corrupted by circular complex Gaussian noise for which the associated deterministic CRLB was easily derived. However, the deterministic CRLB is known to be not achievable in the general case. Hence, there has been interest in developing the stochastic CRB which can be asymptotically achieved by the stochastic ML estimator.

Several works which deal with the computation of the stochastic CRLB have been reported in the litterature. In fact, an explicit expression of the CRLB for real Gaussian distributions was derived in [11, 12] by Slepian and Bangs. This work was extended to circular complex Gaussian distributions in [13]. Although their efficiency, all the oforementioned CRLBs present some practical limitations. In fact, they are mainly developed assuming the snapshots to be iid or uncorrelated in time. This assumption places a challenging limitation on the applicability of the results in the real world and forces some practical difficulties. Therefore, efforts have been directed to consider more realistic models assuming the signals to be temporally correlated. Then, an explicit expression for the stochastic DOA CRLB of circular Gaussian distributed and temporally correlated signals was derived in [6]. Yet, noncircular complex signals, for example binary phase shift keying (BPSK) and offset-quadrature-phase-shift-keying (OQPSK) modulated signals, are frequently encountered in digital communications. Therefore, more recently, an explicit expression for the stochastic DOA CRLB of noncircular Gaussian sources was derived in [14] but for iid signals. But, to the best of our knowledge, no contibutions have dealt yet with the derivation of the DOA CRLB assuming the signals to be both spatially and temporally correlated and also generated from noncircular sources. Therefore, the aim of our proposed work is to derive an explicit expression of the CRB of the DOA estimates assuming spatially and temporally correlated signals generated from noncircular sources.

This paper is organized as follows. In section II, we present the notations and definitions used throughout the article. In section III, we introduce the system model that will be used to derive the CRB. In section IV, an explicit expression of the DOA CRB assuming spatially and temporally correlated signals generated from noncircular sources will be derived. In section V, some concluding remarks will be drawn out.

II. Notations and definitions

A. Notations

We mention that throughout this paper, matrices and vectors are represented by bold upper case and bold lower case characters, respectively. Vectors are, by default, in column orientation.

$(A)^*$	:	Conjugate of the matrix A
$(A)^T$	:	Transpose of A
$(A)^H$	:	Conjugate transpose of A
$\mathrm{tr}(A)$	:	Trace of A
$\|A\|_{\text{Fro}}$	:	Frobenius norm of A; $\|A\|_{\text{Fro}}^2 = \mathrm{tr}(AA^H)$
$\mathrm{vec}(A)$	:	The "vectorization" operator that turns the matrix A into a vector by stacking the columns of the matrix one below another
$\Re\{.\}$	:	Real part operator
$\Im\{.\}$	:	Imaginary part operator
$\mathrm{E}\{.\}$	:	Expectation operator
$\otimes$	:	The Kronecker operator
$\odot$	:	The Hadamard-Schur product operator
$\boldsymbol{I}_p$	:	The $(p \times p)$ identity matrix
$\mathbf{0}_{p\times q}$	:	The $(p \times q)$ null matrix
$\mathcal{N}(\mathbf{0}, \boldsymbol{P})$	:	A centred normal distribution with first covariance matrix $\boldsymbol{P} = \mathrm{E}\{\boldsymbol{x}(t)\boldsymbol{x}^H(t)\}$

B. Definitions

We will first define what the true SNR means. In fact, the true SNR of a considered system can be defined as follows:

$$\text{SNR} = \frac{P_{\text{signal}}}{P_{\text{noise}}}, \tag{1}$$

where P_{signal} is the power of the transmitted signal and P_{noise} is the power of the noise.

Now, to define the noncircularity rate and the noncircularity phase notions, we denote Z ($\boldsymbol{Z}$, respectively) a centred random variable (a centred random vector, respectively). In this paper, we consider as second-order noncircular (NC), the random variables (vectors, respectively) such as $\mathrm{E}\{Z^2\} \neq 0$ ($\mathrm{E}\{\boldsymbol{Z}\boldsymbol{Z}^T\} \neq 0$, respectively).

The degree of second-order noncircularity of a centred random variable Z is determined by the noncircularity rate ρ of module lower than 1 defined as follows

$$\frac{\mathrm{E}\{Z^2\}}{\mathrm{E}\{|Z|^2\}} = \rho e^{i\phi},$$

where the parameter ϕ represents the noncircularity phase.

III. System Model

Consider an array of L sensors receiving the signals emitted by K narrowband sources with directions $\boldsymbol{\theta} = (\theta_1, \ldots, \theta_K)$. Then, the received data can be modelled as a complex signal as follows:

$$\boldsymbol{y}(t) = \boldsymbol{A}\ \boldsymbol{x}(t) + \boldsymbol{w}(t), \quad t = 1, 2, \ldots, N, \tag{2}$$

where, N represents the total number of received samples in the observation window. At time index t, $\boldsymbol{x}(t)$ is the transmitted sources signals, $\boldsymbol{A} = (\boldsymbol{a}(\theta_1), \ldots, \boldsymbol{a}(\theta_K))$ is the steering matrix with $\{\boldsymbol{a}(\theta_i)\}_{i=1,\ldots,K}$ are the array steering vectors parametrized by the scalar DOA parameters $\{\theta_i\}_{i=1,\ldots,K}$ and $\boldsymbol{w}(t)$ is the sensors noise vector.

Stacking the received data over the whole observation window in a matrix $\boldsymbol{Y}$, (2) can be written in a matrix form as follows:

$$\boldsymbol{Y} = \boldsymbol{A}\ \boldsymbol{X} + \boldsymbol{W}, \tag{3}$$

where $\boldsymbol{Y} = [\boldsymbol{y}(1), \ldots, \boldsymbol{y}(N)]$ represents the data samples, $\boldsymbol{X} = [\boldsymbol{x}(1), \ldots, \boldsymbol{x}(N)]$ is the signal sequence and $\boldsymbol{W} = [\boldsymbol{w}(1), \ldots, \boldsymbol{w}(N)]$ is the noise sequence.

Now, consider that the transmitted signals $\boldsymbol{x}(t)$ are assumed to be generated from noncircular sources. This means that $\mathrm{E}\{\boldsymbol{x}(t)\boldsymbol{x}^T(t)\} \neq 0$ contrarily to circular signals. Otherwise, the transmitted signals $\{\boldsymbol{x}(t)\}_{t=1,2,\ldots,N}$ are supposed to be

978-1-4244-8840-7/10/$26.00©2010 IEEE

zero-mean complex noncircular, temporally and possibly spatially correlated with conjugated and unconjugated covariance matrices $\boldsymbol{\mathcal{P}}_{NK\times NK}$ and $\boldsymbol{\mathcal{P}}'_{NK\times NK}$, respectively as follows

$$\boldsymbol{\mathcal{P}}_{NK\times NK} = \text{Block}_{ik}[\boldsymbol{\mathcal{P}}^{ik}_{K\times K}], \quad (4)$$
$$\boldsymbol{\mathcal{P}}'_{NK\times NK} = \text{Block}_{ik}[\boldsymbol{\mathcal{P}}'^{ik}_{K\times K}], \quad (5)$$

where $\text{Block}_{ik}[\boldsymbol{\mathcal{P}}^{ik}_{K\times K}]$ and $\text{Block}_{ik}[\boldsymbol{\mathcal{P}}'^{ik}_{K\times K}]$ represent block matrices with blocks $\boldsymbol{\mathcal{P}}^{ik}_{K\times K}$ and $\boldsymbol{\mathcal{P}}'^{ik}_{K\times K}$ respectively. The ik'th block of the block matrix $\boldsymbol{\mathcal{P}}$, $\boldsymbol{\mathcal{P}}^{ik}$, represents the first space-time covariance matrix of the signals and is defined as

$$\boldsymbol{\mathcal{P}}^{ik} = \boldsymbol{P}_{ik}, \quad (6)$$
$$= \text{E}\{\boldsymbol{x}(i)\boldsymbol{x}^H(k)\}. \quad (7)$$

Moreover, the ik'th block of the block matrix $\boldsymbol{\mathcal{P}}'$, $\boldsymbol{\mathcal{P}}'^{ik}$, represents the second unconjugated spatial covariance matrix of the signals and is defined as

$$\boldsymbol{\mathcal{P}}'^{ik} = \boldsymbol{P}'_{ik}, \quad (8)$$
$$= \text{E}\{\boldsymbol{x}(i)\boldsymbol{x}^T(k)\}. \quad (9)$$

The noise is assumed to be Gaussian complex circular, possibly spatially correlated and temporally white. Therefore, we have

$$\text{vec}(\boldsymbol{W}) \sim \mathcal{N}(\boldsymbol{0}, \boldsymbol{\mathcal{C}}), \quad (10)$$

where

$$\boldsymbol{\mathcal{C}} = \boldsymbol{I}_N \otimes \boldsymbol{C}. \quad (11)$$

$\boldsymbol{C}$ represents the noise covariance matrix defined as follows

$$\boldsymbol{C} = \text{E}\{\boldsymbol{w}(t)\boldsymbol{w}^H(t)\}. \quad (12)$$

Therefore, the received signals are zero-mean complex noncircular, temporally and possibly spatially correlated with conjugated and unconjugated covariance matrices $\boldsymbol{\mathcal{R}}_{NL\times NL}$ and $\boldsymbol{\mathcal{R}}'_{NL\times NL}$, respectively as follows

$$\boldsymbol{\mathcal{R}}_{NL\times NL} = \boldsymbol{\mathcal{A}}\boldsymbol{\mathcal{P}}\boldsymbol{\mathcal{A}}^H + \boldsymbol{\mathcal{C}}, \quad (13)$$
$$\boldsymbol{\mathcal{R}}'_{NL\times NL} = \boldsymbol{\mathcal{A}}\boldsymbol{\mathcal{P}}\boldsymbol{\mathcal{A}}^T, \quad (14)$$

where

$$\boldsymbol{\mathcal{A}} = \boldsymbol{I}_N \otimes \boldsymbol{A}. \quad (15)$$

In this paper, we consider the same assumptions $A1$, $A2$ and $A3$ recently introduced in [6] as follows:

- A1) It is assumed that $K < L$ and that for any set of distinct DOA parameters $\theta_1, \ldots, \theta_L$, the vectors $\{\boldsymbol{a}(\theta_1), \ldots, \boldsymbol{a}(\theta_L)\}$ are linearly independent. Furthermore, $\boldsymbol{a}(\theta)$ is assumed to be differentiable with respect to θ and the true parameter vector $\boldsymbol{\theta}_0$ is an inner point of the set of parameter vectors of interest.
- A2) The transmitted signals $\{\boldsymbol{x}(t)\}_{t=1,2,\ldots,N}$ are assumed to be independent from the noise components $\{\boldsymbol{w}(t)\}_{t=1,2,\ldots,N}$.
- A3) The signals are assumed to exhibit a "sufficient" temporal correlation.

IV. Derivation of the CRB for noncircular Gaussian distributed and temporally correlated signals

In this section, we assume that the transmitted signals $\{\boldsymbol{x}(t)\}_{t=1,2,\ldots,N}$ are zero-mean Gaussian distributed. Then, we introduce the following extended vector $\widetilde{\boldsymbol{x}}$

$$\widetilde{\boldsymbol{x}} = \begin{pmatrix} \boldsymbol{x} \\ \boldsymbol{x}^* \end{pmatrix}. \quad (16)$$

Then, we have

$$\widetilde{\boldsymbol{x}} \sim \mathcal{N}(\boldsymbol{0}, \widetilde{\boldsymbol{\mathcal{P}}}), \quad (17)$$

where

$$\widetilde{\boldsymbol{\mathcal{P}}} = \text{E}\left\{\widetilde{\boldsymbol{x}}\widetilde{\boldsymbol{x}}^H\right\}, \quad (18)$$
$$= \begin{pmatrix} \boldsymbol{\mathcal{P}} & \boldsymbol{\mathcal{P}}' \\ \boldsymbol{\mathcal{P}}'^* & \boldsymbol{\mathcal{P}}^* \end{pmatrix}, \quad (19)$$

where $\boldsymbol{\mathcal{P}}$ and $\boldsymbol{\mathcal{P}}'$ are previously defined in (4) and (5), respectively.

To derive the CRB of the considered model, we assume that the noise is circular Gaussian distributed and the noise covariance matrix $\boldsymbol{C}$ is known (possibly up to a multiplicative scalar). Then, we define the parameter vector as follows

$$\boldsymbol{\alpha} = \left(\boldsymbol{\theta}^T, \boldsymbol{\beta}^T\right)^T, \quad (20)$$

where $\boldsymbol{\theta}$ introduced in section II represents the directions of the narrowband sources and $\boldsymbol{\beta}$ is defined by

$$\boldsymbol{\beta} = \Big(\left(\Re\{\boldsymbol{P}_{ij}\}, \Im\{\boldsymbol{P}_{ij}\}, \Re\{\boldsymbol{P}'_{ij}\}, \Im\{\boldsymbol{P}'_{ij}\}\right)_{1\le j<i\le NK}, \left(\boldsymbol{P}_{ii}, \Re\{\boldsymbol{P}'_{ii}\}, \Im\{\boldsymbol{P}'_{ii}\}\right)_{i=1,\ldots,NK}\Big)^T. \quad (21)$$

We also define the vector $\overline{\boldsymbol{y}}_N$ as

$$\overline{\boldsymbol{y}}_N = \begin{pmatrix} \boldsymbol{C}^{-\frac{1}{2}}\boldsymbol{y}(1) \\ \vdots \\ \boldsymbol{C}^{-\frac{1}{2}}\boldsymbol{y}(N) \end{pmatrix}. \quad (22)$$

Moreover, we introduce the following extended vector $\widetilde{\overline{\boldsymbol{y}}}_N$

$$\widetilde{\overline{\boldsymbol{y}}}_N = \begin{pmatrix} \overline{\boldsymbol{y}}_N \\ \overline{\boldsymbol{y}}_N^* \end{pmatrix}. \quad (23)$$

Then, we have

$$\widetilde{\overline{\boldsymbol{y}}}_N \sim \mathcal{N}(\boldsymbol{0}, \widetilde{\boldsymbol{\mathcal{R}}}_N), \quad (24)$$

where

$$\widetilde{\boldsymbol{\mathcal{R}}}_N = \text{E}\left\{\widetilde{\overline{\boldsymbol{y}}}_N \widetilde{\overline{\boldsymbol{y}}}_N^H\right\}, \quad (25)$$
$$= \begin{pmatrix} \boldsymbol{\mathcal{R}}_N & \boldsymbol{\mathcal{R}}'_N \\ \boldsymbol{\mathcal{R}}'^*_N & \boldsymbol{\mathcal{R}}^*_N \end{pmatrix}, \quad (26)$$

with

$$\boldsymbol{\mathcal{R}}_N = \text{E}\left\{\overline{\boldsymbol{y}}_N \overline{\boldsymbol{y}}_N^H\right\}, \quad (27)$$
$$\boldsymbol{\mathcal{R}}'_N = \text{E}\left\{\overline{\boldsymbol{y}}_N \overline{\boldsymbol{y}}_N^T\right\}. \quad (28)$$

$\mathcal{R}_N$ and $\mathcal{R}'_N$ can be written as

$$\mathcal{R}_N = \overline{G}\mathcal{P}\overline{G}^H + I_{NL}, \quad (29)$$
$$\mathcal{R}'_N = \overline{G}\mathcal{P}'\overline{G}^H, \quad (30)$$

where $\overline{G}$ is defined as follows

$$\overline{G} = I_N \otimes \left(C^{-\frac{1}{2}}A\right). \quad (31)$$

Therefore, $\widetilde{\mathcal{R}}_N$ is rewritten as

$$\widetilde{\mathcal{R}}_N = \widetilde{\overline{G}}\widetilde{\mathcal{P}}\widetilde{\overline{G}}^H + I_{2NL}, \quad (32)$$

where

$$\widetilde{\overline{G}} = \begin{pmatrix} \overline{G} & \mathbf{0}_{NL\times NK} \\ \mathbf{0}_{NL\times NK} & \overline{G}^* \end{pmatrix}.$$

Similarly to [14], the ik'th entry of the Fisher information matrix (FIM) corresponding to $\widetilde{\overline{y}}_N$ is given by

$$(I_{\rm F})_{ik} = ({\rm CRB})^{-1}_{ik}, \quad (33)$$
$$= \frac{1}{2}{\rm tr}\left(\frac{\partial\widetilde{\mathcal{R}}_N}{\partial\alpha_i}\widetilde{\mathcal{R}}_N^{-1}\frac{\partial\widetilde{\mathcal{R}}_N}{\partial\alpha_k}\widetilde{\mathcal{R}}_N^{-1}\right). \quad (34)$$

Following the same steps of [10], we obtain the following expression of the $\left({\rm CRB}^{-1}\right)_{ik}$

$$\left({\rm CRB}^{-1}(\theta)\right)_{ik} = \Re\left\{{\rm tr}\left(\widetilde{\overline{G}}_i^H \Pi^{\perp}_{\widetilde{\overline{G}}}\widetilde{\overline{G}}_k\widetilde{\mathcal{P}}\,\widetilde{\overline{G}}^H\widetilde{\mathcal{R}}_N^{-1}\,\widetilde{\overline{G}}\,\widetilde{\mathcal{P}}\right)\right\}, \quad (35)$$

where

$$\widetilde{\overline{G}}_i = \frac{{\rm d}\widetilde{\overline{G}}(\theta)}{{\rm d}\theta_i}, \quad (36)$$
$$\Pi^{\perp}_{\widetilde{\overline{G}}} = I_{2NL} - \widetilde{\overline{G}}\left(\widetilde{\overline{G}}^H\widetilde{\overline{G}}\right)^{-1}\widetilde{\overline{G}}^H. \quad (37)$$

Some algebraic manipulations (see appendix A) yield the following expression of ${\rm CRB}(\theta)$ for temporally correlated signals generated from noncircular sources

$${\rm CRB}^{\rm noncir/cor}(\theta) = \frac{1}{2}\left[\Re\left\{\left(D^H C^{-\frac{1}{2}}\Pi^{\perp}_{G}C^{-\frac{1}{2}}D\right)\odot {\rm Btr}_K\left(\left(\begin{pmatrix}\mathcal{P}\mathcal{A}^H & \mathcal{P}'\mathcal{A}^T\end{pmatrix}\widetilde{\mathcal{R}}^{-1}\begin{pmatrix}\mathcal{A}\mathcal{P} \\ \mathcal{A}^*\mathcal{P}'^*\end{pmatrix}\right)\right)^T\right\}\right]^{-1}, \quad (38)$$

where $\mathcal{A}$ is defined in (15) and ${\rm Btr}_K$ denotes the block trace and is defined as

$${\rm Btr}_K(\mathcal{P}) = \sum_i \mathcal{P}^{ii}_{K\times K}. \quad (39)$$

We note here that in the case of circular sources, we have $\mathcal{P}' = \mathbf{0}_{KN\times KN}$ and $\mathcal{R}' = \mathbf{0}_{LN\times LN}$. Therefore, $\widetilde{\mathcal{R}}$ becomes

$$\widetilde{\mathcal{R}} = \begin{pmatrix} \mathcal{R} & \mathbf{0}_{LN\times LN} \\ \mathbf{0}_{LN\times LN} & \mathcal{R}^* \end{pmatrix}. \quad (40)$$

Consequently, (38) reduces to

$${\rm CRB}^{\rm cir/cor}(\theta) = \frac{1}{2}\left[\Re\left\{\left(D^H C^{-\frac{1}{2}}\Pi^{\perp}_{G}C^{-\frac{1}{2}}D\right)\odot {\rm Btr}_K\left(\mathcal{P}\mathcal{A}^H\mathcal{R}^{-1}\mathcal{A}\mathcal{P}\right)^T\right\}\right]^{-1}, \quad (41)$$

derived in [6].

Now, we denote

$$B_1 = \begin{pmatrix}\mathcal{P}\mathcal{A}^H & \mathcal{P}'\mathcal{A}^T\end{pmatrix}\widetilde{\mathcal{R}}^{-1}\begin{pmatrix}\mathcal{A}\mathcal{P} \\ \mathcal{A}^*\mathcal{P}'^*\end{pmatrix}, \quad (42)$$
$$B_2 = \mathcal{P}\mathcal{A}^H\mathcal{R}^{-1}\mathcal{A}\mathcal{P}, \quad (43)$$
$$B_3 = D^H C^{-\frac{1}{2}}\Pi^{\perp}_{G}C^{-\frac{1}{2}}D. \quad (44)$$

Applying [1, lemma A.4] to B_1 and B_2, we obtain

$$B_1 \geq B_2, \quad (45)$$

where for two matrices A and B, $A \geq B$ implies that $A - B \geq \mathbf{0}$. This inequality applies to the transpose of these matrices. Then, we have

$$B_1^T - B_2^T \geq \mathbf{0}. \quad (46)$$

Moreover, we have

$$B_3 \geq \mathbf{0}. \quad (47)$$

Therefore, thanks to standard results of linear algebra (see [15, App. A, result R.19]), we prove the following result

$${\rm CRB}^{\rm noncir/cor}(\theta) \leq {\rm CRB}^{\rm cir/cor}(\theta). \quad (48)$$

V. Illustrative simulations

In this section, we will present some figures showing the Cramer-Rao bounds. We will see that the CRB obtained assuming both noncircular sources and temporally correlated signals is lower than the CRBs derived considering only one of these two assumptions.

We first consider two complex noncircular Gaussian signals with identical noncircularity rate $\rho = 1$ and noncircularity phases $\phi_1 = \pi/2$ and $\phi_2 = \pi/3$. These sources, located at angles $\theta_1 = 0$ and $\theta_2 = 0.2$ radians with respect to the normal of array broadside, impinge on a uniform linear array of 4 sensors separated by a half-wavelength for which $a(\theta_k) = \left[1, e^{j\pi\sin(\theta_k)}, e^{2j\pi\sin(\theta_k)}, \ldots, e^{j(L-1)\pi\sin(\theta_k)}\right]^T$ where $\{\theta_k\}_{k=1,2}$ are the DOAs relative to the normal of the array broadside. We assume that SNR = 0 dB. Moreover, we suppose that the signals are spatially uncorrelated.

To represent the CRBs, we define the first and the second (unconjugated) signal space-time covariance matrices as follows

$$\mathcal{P} = P_t \otimes P, \quad (49)$$
$$\mathcal{P}' = P_t \otimes P', \quad (50)$$

where P and P' are the covariance matrices of the noncircular complex Gaussian signal. Moreover, P_t represents the temporal correlation matrix. We also consider the following expressions of the three matrices as follows

$$(\boldsymbol{P})_{ik} = \delta_{ik}, \quad (51)$$
$$(\boldsymbol{P}')_{ik} = \rho e^{j\phi_i}\delta_{ik}, \quad (52)$$
$$(\boldsymbol{P}_t)_{ik} = e^{-0.2|i-k|}. \quad (53)$$

Otherwise, we define the noise covariance matrix as follows

$$(\boldsymbol{C})_{ik} = \sigma^2 e^{|i-k|}. \quad (54)$$

Figs. 1 and 2 show $\ln(\text{CRB}^{\text{noncir/cor}})$, $\ln(\text{CRB}^{\text{cir/cor}})$, $\ln(\text{CRB}^{\text{noncir/uncor}})$ and the deterministic CRB $\ln(\text{CRB}^{\text{det}})$ as a function of the number of snapshots N. From Figs. 1 and 2, we verify that

$$\text{CRB}^{\text{det}} \leq \text{CRB}^{\text{noncir/cor}} \leq \text{CRB}^{\text{cir/cor}}, \quad (55)$$
$$\text{CRB}^{\text{noncir/cor}} \leq \text{CRB}^{\text{noncir/uncor}}. \quad (56)$$

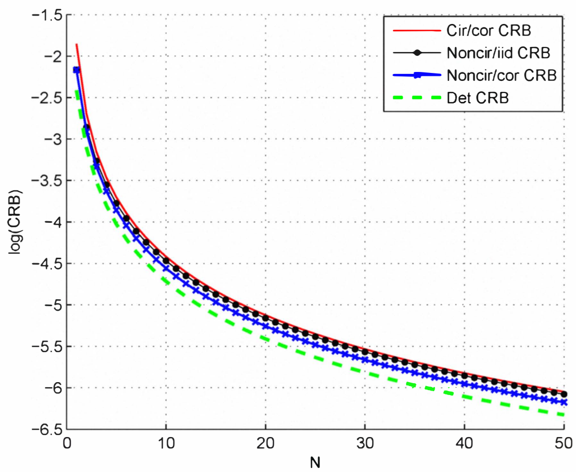

Figure 1. An example of the CRBs versus the number of snapshots N in logarithmic scale for two equipowered sources.

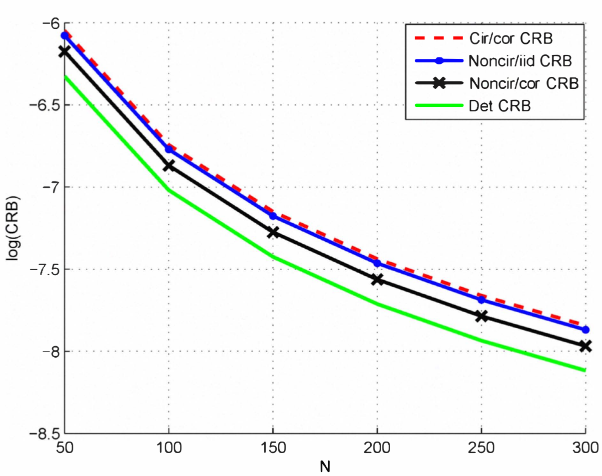

Figure 2. CRBs versus the number of snapshots N in logarithmic scale for two equipowered sources.

We verify also that the CRB obtained assuming both noncircular sources and temporally correlated signals is lower than the CRBs derived considering only one of these two assumptions. This illustrates the potential gain that both the noncircularity and the temporal correlation offer when considered together. Moreover, we see, from Figs. 1 and 2, that the difference between these CRBs increases with the number of snapshots N. This is hardly surprising since the more samples we receive, the more information we can retrieve about the temporal correlation and the noncircularity of the signals. In fact, with increased number of snapshots N, there is more room for both the noncircularity of the signals and the temporal correlation to improve the DOA estimation performance. Now, we consider, in Fig. 3, three equipowered sources with identical noncircularity rate $\rho = 1$ and noncircularity phases $\phi_1 = \pi/2$, $\phi_2 = \pi/2$ and $\phi_3 = \pi/3$. These sources are located at angles $\theta_1 = 0$, $\theta_2 = 0.2$ and $\theta_3 = 0.4$ radians. Fig. 3 illustrates the inequalities (55) and (56). Moreover, it

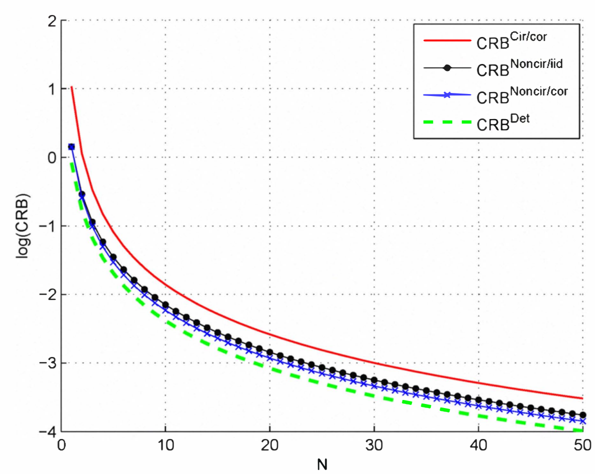

Figure 3. An example of the CRBs versus the number of snapshots N in logarithmic scale for three equipowered sources.

proves that the difference between $\text{CRB}^{\text{noncir/cor}}$ and $\text{CRB}^{\text{cir/cor}}$ increases with the number of sources K while the difference between $\text{CRB}^{\text{noncir/cor}}$ and $\text{CRB}^{\text{noncir/noncor}}$ decreases as K increases. This can be explained by the fact that with increased K, there is more room for the noncircularity of the signals to improve the DOA estimation performance than the temporal correlation.

In the following graphical representations, we consider the case of two equipowered sources. In Fig. 4, the CRBs are depicted versus the SNR for a number of snapshots $N = 100$. It can be seen, from this figure, that as the SNR increases, the CRBs merge together and decrease linearly. In fact, at high SNR values, the useful signals are not too much corrupted by

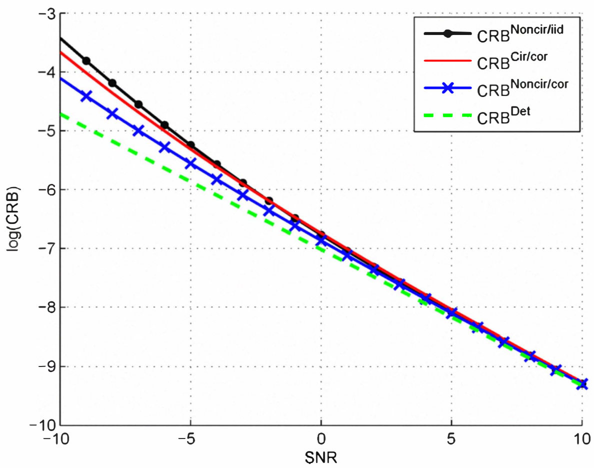

Figure 4. An example of the CRBs versus the SNR in logarithmic scale for two equipowered sources and number of snapshots $N = 100$.

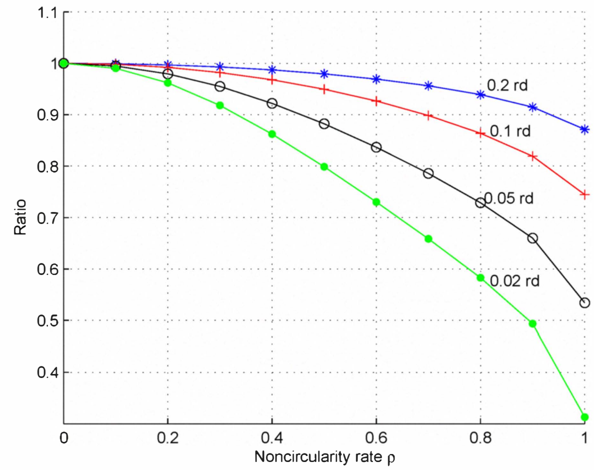

Figure 5. Ratio $= \left(\text{CRB}^{\text{noncir/cor}}\right) / \left(\text{CRB}^{\text{cir/cor}}\right)$ as a function of the noncircularity rate ρ for different values of DOA separation $(\Delta\theta)$, for $\phi_1 = \pi/2$, $\phi_2 = \pi/3$, $N = 100$ and $SNR = 0dB$.

noise. Then, in this SNR region, the signals are very informative about the the DOA estimates. This scenario is therefore equivalent to the deterministic case. This illustrates the fact that at high SNR values, all the CRBs coincide. Moreover, we notice that at low SNR values the temporal correlation is more informative about the unknown DOA parameters than the noncircularity. In fact, at low SNR values, the useful signals are too much corrupted by the noise. Therefore, the useful signals are not very informative about the unknown DOA and more particularly, the noncircularity rate does not bring much information about the DOA estimates.

In Figs. 5 and 6, we show the dependence of the $\text{CRB}^{\text{noncir/cor}}$ on the noncircularity rate ρ , the circularity phase separation $\Delta\phi = \phi_2 - \phi_1$ and the DOA separation $\Delta\theta = \theta_2 - \theta_1$.

In fact, Fig. 5 represents the ratio $\left(\text{CRB}^{\text{noncir/cor}}\right) / \left(\text{CRB}^{\text{cir/cor}}\right)$ as a function of the noncircularity rate for different values of $\Delta\theta$ for $N = 100$ and $SNR = 0dB$. It can be seen from this figure that $\text{CRB}^{\text{noncir/cor}}$ decreases as the noncircularity rate increases. Furthermore, this decrease is more prominent at low DOA separations. Moreover, from Fig. 6, we see that the $\text{CRB}^{\text{noncir/cor}}$ is sensitive to the circularity phase separation at low DOA separations.

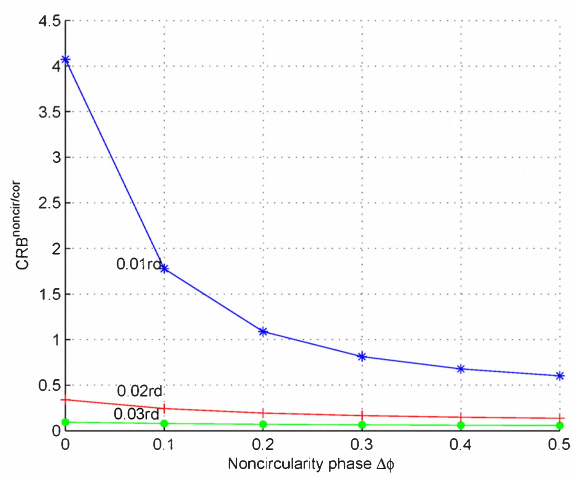

Figure 6. $\text{CRB}^{\text{noncir/cor}}$ as a function of the noncircularity phase $\Delta\phi$ for different values of DOA separation $(\Delta\theta)$, for $\rho = 1$, $N = 100$ and $SNR = 0dB$.

VI. Conclusion

In this paper, we derived for the first time an explicit expression for the stochastic Cramér-Rao bound (CRB) of the DOA estimates for spatially and temporally correlated signals generated from noncircular sources. This CRB was compared to those of circular temporally correlated and noncircular independent and identically distributed signals. We showed the potential gain that both the noncircularity and the temporal correlation provide when considered together. We also proved that the difference between the three CRBs increases with the number of snapshots. On the other hand, as SNR increases, the CRBs merge together and decrease linearly. Otherwise, we showed that at low SNR values the temporal correlation is more informative about the unknown DOA parameters than the noncircularity. Finally, we proved that the CRB derived assuming noncircular and temporally correlated signals decreases as the noncircularity rate increases. Furthermore, this decrease is more prominent at low DOA separations. Moreover, this CRB is sensitive to the noncircularity phase separation at low DOA separations.

APPENDIX A-PROOF OF (38)

We have

$$\left(\mathrm{CRB}^{-1}(\boldsymbol{\theta})\right)_{ik} = \Re\left\{\mathrm{tr}\left(\widetilde{\overline{G}}_i^H \boldsymbol{\Pi}^{\perp}_{\widetilde{\overline{G}}} \widetilde{\overline{G}}_k \widetilde{\mathcal{P}}\, \widetilde{\overline{G}}^H \widetilde{\mathcal{R}}_N^{-1}\, \widetilde{\overline{G}}\, \widetilde{\mathcal{P}}\right)\right\}. \tag{57}$$

This expression is equivalent to

$$\left(\mathrm{CRB}^{-1}(\boldsymbol{\theta})\right)_{ik} = \Re\left\{\mathrm{tr}\left(\begin{pmatrix} \overline{G}_i^H \boldsymbol{\Pi}^{\perp}_{\overline{G}} \overline{G}_k & \mathbf{0} \\ \mathbf{0} & \overline{G}_i^T \boldsymbol{\Pi}^{\perp *}_{\overline{G}} \overline{G}_k^* \end{pmatrix} \times \begin{pmatrix} \mathcal{P}\,\overline{G}^H & \mathcal{P}'\,\overline{G}^T \\ \mathcal{P}'^*\,\overline{G}^H & \mathcal{P}^*\,\overline{G}^T \end{pmatrix} \widetilde{\mathcal{R}}_N^{-1} \begin{pmatrix} \overline{G}\,\mathcal{P} & \overline{G}\,\mathcal{P}' \\ \overline{G}^*\,\mathcal{P}'^* & \overline{G}^*\,\mathcal{P}^* \end{pmatrix}\right)\right\}. \tag{58}$$

Observing that

$$\boldsymbol{\Pi}^{\perp}_{\widetilde{\overline{G}}} = \boldsymbol{I}_N \otimes \boldsymbol{\Pi}^{\perp}_{\overline{G}}, \tag{59}$$

we get

$$\left(\mathrm{CRB}^{-1}(\boldsymbol{\theta})\right)_{ik} = 2\Re\left\{\mathrm{tr}\left(\left(\boldsymbol{I}_N \otimes \boldsymbol{D}_i^H \boldsymbol{C}^{-\frac{1}{2}} \boldsymbol{\Pi}^{\perp}_{\boldsymbol{G}} \boldsymbol{C}^{-\frac{1}{2}} \boldsymbol{D}_k\right) \times \begin{pmatrix} \mathcal{P}\,\overline{G}^H & \mathcal{P}'\,\overline{G}^T \end{pmatrix} \widetilde{\mathcal{R}}_N^{-1} \begin{pmatrix} \overline{G}\,\mathcal{P} \\ \overline{G}^*\,\mathcal{P}'^* \end{pmatrix}\right)\right\}, \tag{60}$$

where

$$\boldsymbol{D}_i = \mathrm{d}\boldsymbol{A}(\boldsymbol{\theta})/\mathrm{d}\theta_i. \tag{61}$$

We also consider that

$$\boldsymbol{D} = (\boldsymbol{d}_1, \ldots, \boldsymbol{d}_K), \tag{62}$$

where

$$\boldsymbol{d}_i = \mathrm{d}\boldsymbol{a}(\theta_i)/\mathrm{d}\theta_i, \quad i = 1, 2, \ldots, K. \tag{63}$$

Then, $\boldsymbol{D}_i$ can be written as

$$\boldsymbol{D}_i = (\mathbf{0}_{L\times 1}, \ldots, \boldsymbol{d}_i, \ldots, \mathbf{0}_{L\times 1}). \tag{64}$$

Therefore, $\left(\mathrm{CRB}^{-1}(\boldsymbol{\theta})\right)_{ik}$ can be written as

$$\left(\mathrm{CRB}^{-1}(\boldsymbol{\theta})\right)_{ik} = 2\Re\left\{\sum_{j=1}^{N}\left(\boldsymbol{d}_i^H \boldsymbol{C}^{-\frac{1}{2}} \boldsymbol{\Pi}^{\perp}_{\boldsymbol{G}} \boldsymbol{C}^{-\frac{1}{2}} \boldsymbol{d}_k\right)\{\boldsymbol{F}_j\}_{ki}\right\}, \tag{65}$$

where $\boldsymbol{F}_j$ represents the $j^{\text{th}}(K \times K)$ block on the diagonal of the matrix $\begin{pmatrix} \mathcal{P}\,\overline{G}^H & \mathcal{P}'\,\overline{G}^T \end{pmatrix} \widetilde{\mathcal{R}}_N^{-1} \begin{pmatrix} \overline{G}\,\mathcal{P} \\ \overline{G}^*\,\mathcal{P}'^* \end{pmatrix}$. Consequently, we obtain the following expression of $\mathrm{CRB}^{-1}(\boldsymbol{\theta})$

$$\mathrm{CRB}^{-1}(\boldsymbol{\theta}) = 2\Re\left\{\sum_{j=1}^{N}\left(\boldsymbol{D}^H \boldsymbol{C}^{-\frac{1}{2}} \boldsymbol{\Pi}^{\perp}_{\boldsymbol{G}} \boldsymbol{C}^{-\frac{1}{2}} \boldsymbol{D}\right) \odot \boldsymbol{F}_j^T\right\}. \tag{66}$$

We use this following identity

$$\widetilde{\mathcal{R}}_N = \widetilde{\mathcal{C}}^{-\frac{1}{2}} \widetilde{\mathcal{R}} \widetilde{\mathcal{C}}^{-\frac{1}{2}}, \tag{67}$$

where

$$\widetilde{\mathcal{R}} = \begin{pmatrix} \mathcal{R} & \mathcal{R}' \\ \mathcal{R}'^* & \mathcal{R}^* \end{pmatrix}, \tag{68}$$

with $\mathcal{R}$ and $\mathcal{R}'$ are previously defined in (13) and (14), respectively. Then, after some algebraic manipulations, we obtain the expression of $\mathrm{CRB}^{\mathrm{cor/noncir}}(\boldsymbol{\theta})$ as given by (38).

REFERENCES

[1] P. Stoica, and A. Nehorai, "Performance Study of Conditional and Unconditional Direction-of-Arrival Estimation," *IEEE Trans. Acoust., Speech, Signal Processing*, vol. 38, pp. 1783-1795, Oct. 1990.

[2] P. Stoica and A. Nehorai, "MUSIC, Maximum Likelihood, and Cramer-Rao Bound," *IEEE Trans. Acoust., Speech, Signal Processing*, vol. 37, pp. 720-741, May 1989.

[3] P. Stoica and A. Nehorai, "MUSIC, Maximum Likelihood, and Cramér-Rao Bound:Further Results and Comparisons," *IEEE Trans. Acoust., Speech, Signal Processing*, vol. 38, pp. 2140-2150, Dec. 1990.

[4] D. Slepian, "Maximum Likelihood Methods for Direction-of-Arrival Estimation,"*IEEE Trans. Acoust., Speech, Signal Processing*, vol. 38, pp. 1132-1143, July 1990.

[5] P. Stoica, M. Viberg and B. Ottersten "Instrumental Variable Approach to Array Processing in Spatially Correlated Noise Fields," *IEEE Trans. Sig. Process.*, vol. 42, pp. 121-133, January. 1994.

[6] M. Viberg, P. Stoica, and B. Ottersten "Array Processing in Correlated Noise Fields Based on Instrumental Variables and Subspace Fitting," *IEEE Trans. Sig. Process.*, vol. 43, pp. 1187-1199, May 1995.

[7] J. P. Delmas, "Asymptotically Minimum Variance Second-Order Estimation for Noncircular Signals with Application to DOA Estimation," *IEEE Trans. Sig. Process.*, vol. 52, pp. 1235-1241, May 2004.

[8] H. Abeida and J. P. Delmas, "MUSIC-Like Estimation of Direction of Arrival for Noncircular Sources," *IEEE Trans. Sig. Process.*, vol. 54, pp. 2678-2689, July 2006.

[9] Patrick GOUNON, C. ADNET, and Jérôme GALY, "Angular Localisation for Non Circular Signals," *GRETSI, Saint Martin d'Hères, France*, 1998.

[10] P. Stoica, A. G. Larsson, and A. B. Gershman, "The stochastic CRB for array processing: A textbook derivation," *IEEE Sig. Process. Lett.*, vol. 8, pp. 148-150, May 2001.

[11] D. Slepian, "Estimation of signal parameters in the presence of noise," *Trans. IRE Prof. Group Inform. Theory PG IT-3*, pp. 68-89, 1954.

[12] W. J. Bangs, *Array Processing with Generalized Beamformers*, Ph.D. Dissertation, Yale Univ., New Haven, CT, 1971.

[13] P. Stoica and R. Moses, *Introduction to Spectral Analysis. Upper Saddle River*, NJ: Prentice-Hall, 1997.

[14] J. P. Delmas and H. Abeida, "Stochastic Cramér-Rao Bound for Noncircular Signals with Application to DOA Estimation," *IEEE Trans. Sig. Process.*, vol. 52, pp. 3192-3199, Nov. 2004.

[15] P. Stoica and R. Moses, *Introduction to Spectral Analysis. Upper Saddle River*, NJ: Prentice-Hall, 1997.